# ION IMPLANTATION AND ANNEALING STUDIES IN III-V NITRIDES

J. C. ZOLPER,[a] S. J. PEARTON,[b] J. S. WILLIAMS,[c] H. H. TAN,[c] R. J. KARLICEK,[d] JR., R. A. STALL[d]

[a] Sandia National Laboratories, Albuquerque, NM 87185-0603,
[b] University of Florida, Department of Materials Science and Engineering, Gainesville, FL 32611,
[c] Dept. of Electronic Materials Engineering, Australian National University, Canberra, 0200, Australia,
[d] Emcore Corp., Somerset, NJ 08873

## ABSTRACT

Ion implantation doping and isolation is expected to play an enabling role for the realization of advanced III-Nitride based devices. In fact, implantation has already been used to demonstrate n- and p-type doping of GaN with Si and Mg or Ca, respectively, as well as to fabricate the first GaN junction field effect transistor.[1-4] Although these initial implantation studies demonstrated the feasibility of this technique for the III-Nitride materials, further work is needed to realize its full potential.

After reviewing some of the initial studies in this field, we present new results for improved annealing sequences and defect studies in GaN. First, sputtered AlN is shown by electrical characterization of Schottky and Ohmic contacts to be an effect encapsulant of GaN during the 1100 °C implant activation anneal. The AlN suppresses N-loss from the GaN surface and the formation of a degenerate $n^+$-surface region that would prohibit Schottky barrier formation after the implant activation anneal. Second, we examine the nature of the defect generation and annealing sequence following implantation using both Rutherford Backscattering (RBS) and Hall characterization. We show that for a Si-dose of $1\times10^{16}$ $cm^{-2}$ 50% electrical donor activation is achieved despite a significant amount of residual implantation-induced damage in the material.

MASTER

## INTRODUCTION

The group III-Nitride semiconductors (GaN, AlN, and InN) have become the focus of intense research following the demonstration of high brightness light emitting diodes based first on GaN p/n junctions and more recently based on InGaN quantum wells.[5,6] In addition III-Nitride based laser diodes have also been reported.[7] The impressive photonic device results where achieved in epitaxial III-nitride material grown on sapphire substrates with a lattice mismatch in excess of 12% and with a resulting defect density on the order of $10^{10}$ $cm^{-2}$.[8]

In addition to photonic device demonstrations, these materials are also very attractive for electronic devices that operate at high power or high temperature. Already Heterostructure Field Effect Transistors, Junction Field Effect Transistors, and

# DISCLAIMER

# DISCLAIMER

Portions of this document may be illegible
in electronic image products.  Images are
produced from the best available original
document.

Heterojunction Bipolar Transistors have been demonstrated with impressive properties considering the highly defective nature of these materials.[4,9-14] While continued improvements in epitaxial material quality can be expected to yield improved device results, advances are also needed in device processing technology.
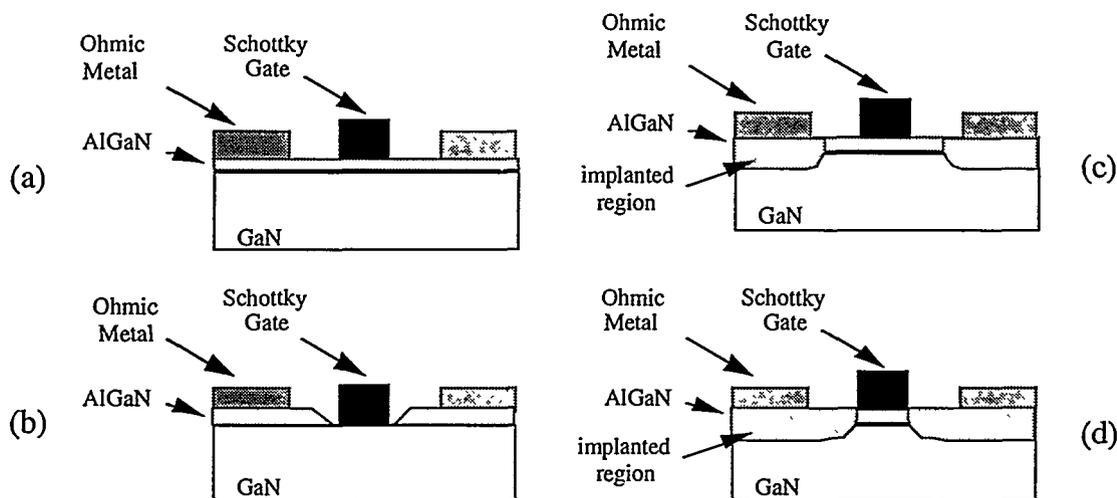


Fig 1. Schematics of typical FET structures a) fully planar with uniform lateral doping, b) recessed gate, c) non-self-aligned, implanted, d) self-aligned, implanted.

One processing technique of particular utility for electronic devices is ion implantation that can be employed for selective area doping or isolation. This is illustrated in Fig 1 with four transistor structures. Fig 1.a shows the fully planar (ignoring possible mesa etching for interdevice isolation) structure that has been employed for the majority of AlGaN/GaN heterostructure field effect transistors (HFETs) reported to date.[9-13] This structure suffers from a high access resistance since the doping is uniform in both the channel and ohmic regions and must therefore be a compromise between the two. An improved structure is the recessed gate approach shown in Fig 2.b that is widely used in other compound semiconductor materials.[15] The recess gate design reduces the access resistance by having a highly doped capping layer that is removed in the gate region, typically by a wet etch process. For the III-Nitride materials, however, no appropriate wet etch chemistry has been identified thus making the use of this structure problematic. Although some success has been reported with dry recess etch processes, control of the plasma damage becomes critical and has limited this approach so far.[16,17] Figure 1c show an alternative approach to realizing higher doping in the ohmic contact regions without impacting the channel. In this case, the contact regions are defined by a photolithographic process and selectively implanted with the appropriate doping species. In this way, no etching of the semiconductor is required. This approach will require the GaN surface to maintain its stiochiometry during the implant activation anneal so that a Schottky contact can be formed for the gate electrode after the activation anneal. Finally, Fig 1d shows a more optimum approach with the source and drain implants self-aligned to the gate Schottky contact metal. This final structure will require the Schottky metal to be in place during the implant activation anneal and to maintain its rectifying properties following the thermal processing. The development of such a high

temperature metallization scheme will be challenging due to the high implant activation annealing temperature (~1100 °C) required for GaN.

In this paper, we review the progress in ion implantation doping of GaN such as would be needed to realize the FET structures of Fig 1c,d. This includes the successful demonstration of n-type doping with Si and p-type doping with Mg and Ca. We address the implant activation annealing sequence and in particular the use of an AlN encapsulation layer to maintain the surface stoichiometry to allow Schottky contact formation. The nature of implantation-induced damage will then be discussed. Finally, we outline areas which need further work if ion implantation is to become a viable technology for application to the group III-Nitride materials.

## IMPLANTATION DOPING OF GaN

Implantation has been used to achieve n-type doping in GaN with both Si and O.[1,2] For Si-implantation in Ref 1, although the unimplanted sample showed a reduction in sheet resistance that may be due to the formation of N-vacancies or the depassivation of unintentional impurities, the Si-implanted samples demonstrated a 3 order-of-magnitude decrease in resistance after annealing out to 1100 °C where the Si is becoming an active donor. This result was the first to demonstrate that the activation temperature for implanted dopants in GaN was > 1000 °C. The implant activation temperature of other common compound semiconductors are summarized in Table I and compared to the melting point of the material. For Si, GaSb, InP, and GaAs the implant activation temperature is seen to be roughly 70% for the melting point while for SiC and GaN it is closer to 50%. This suggests that the optimum implant activation temperature for GaN may be closer to 1700 °C. This hypothesis is support by damage studies presented later in this paper.

**Table I**
Comparison of the melting point and implant activation temperature for the materials listed.

| material | $T_{mp}$ (°C) | $T_{act}$ (°C) | $T_{act}$ (°C)/$T_{mp}$ (°C) |
|----------|---------------|----------------|-------------------------------|
| Si       | 1415          | 950            | 0.67                          |
| GaSb     | 707           | 550            | 0.77                          |
| InP      | 1057          | 750            | 0.71                          |
| GaAs     | 1237          | 850            | 0.69                          |
| SiC      | 2797          | 1300-1600      | 0.46-0.57                     |
| GaN      | 2518          | 1100           | 0.44                          |

The nature of the Si-activation process in GaN is thought to be dominated by a substitutional diffusion process of the host elements with a activation energy of 6.7 eV.[3] This means that the Si-ions are substitutional on Ga-sites at relatively low temperatures but only become electrically active when the anti-site defects ($N_{Ga}$, $Ga_N$) are annihilated.

A primary limitation of the III-Nitride materials, and all wide bandgap semiconductors in general, has been the high ionization energy of acceptor species which significantly limits the number of ionized free holes at room temperature. To date, the

shallowest acceptor in GaN is Mg with an ionization energy level of 150 to 170 meV.[18] Therefore, the search for an alternative acceptor species that has a lower ionization energy is of particular interest. In the regard, implantation has the flexibility to introduce a wide array of elements into the semiconductor lattice to study their properties. Once p-type implantation doping of GaN was demonstrated with Mg with the use of a P co-implantation scheme,[1] other potential acceptor species were studied. The first example of this was Ca-implant doping of GaN where Ca was shown to be an acceptor in GaN. Ca was studied since it had been suggested to be a shallow acceptor in GaN.[19] Both Ca-only and Ca+P samples were examined with both seen to convert from n-type to p-type after an 1100 °C anneal. From an Arrhenius plot of the sheet hole concentration for the Ca-implanted samples annealed at 1150 °C, the ionization energy of Ca in GaN is estimated to be 169 meV or equivalent to that of Mg.[1] Further work to use implantation to identify alternative acceptor species for GaN is on going. To date, two other attractive elements, Be and C, have been investigated by implantation without p-type conductivity being achieved either with or with a co-implantation scheme. It may be that these lighter elements will require a different ratio of co-implant ion to acceptor ion dose than that used for Mg and Ca of 1:1. Alternatively, there may be other defect or impurity interactions, such as complex formation (Be:O in Refs. 20,21 or C:N in Ref. 22), that compensate these elements but do not occur for implanted Mg or Ca. This areas of alternative dopant species requires further study.

## AlN ENCAPSULATION DURING ANNEALING

As discussed above, to realize the FET structure shown in Fig. 1c, the surface stiochiometry of GaN must be maintained during the high temperature activation anneal. To address this problem in other compound semiconductors encapsulation of the surface with a dielectric film is often employed.[23] For this approach to be effective for GaN, the encapsulating film must maintain its integrity (i.e. not crack or blister) and suppress out-diffusion at a temperature of ~1100 °C. Although $SiO_2$ and SiN are typically used for encapsulating other compound semiconductors, they are not viable at these high temperatures due to cracking or hydrogen desorption.[24] AlN, on the other hand, has excellent thermal and mechanical stability even at these high temperatures and can be readily deposited by sputtering Al in a nitrogen ambient. Therefore, sputtered AlN was investigated as an annealing cap for GaN.[25]

Two sets of GaN samples were processed into Pt/Au Schottky contacts following a 1100 °C, 15 s rapid thermal anneal. One set of samples (A-samples) was n-type as-grown (n ~ $1x10^{17}$ $cm^{-3}$) while the second set (B-samples) were initially semi-insulating and was implanted with Si-ions at an energy of 100 keV and a dose of $5x10^{13}$ $cm^{-2}$ to simulate a MESFET channel implant. One sample from each set was encapsulated with 120 nm of reactivity sputtered AlN prior to annealing. Following annealing, the AlN was removed in a selective KOH-based etch (AZ400K developer) at 60-70 °C.[26] This etch has been shown to etch AlN at rates of 60 to 10,000 Å/min, depending on the film quality, while under the same conditions no measurable etching of GaN was observed.[27] The etch rate of the sputter deposited AlN film was found to increase as a function of post-deposition annealing temperature.[28] Ti/Al ohmic contacts were deposited and defined by conventional lift-off techniques on all samples and annealed at 500 °C for 15 s. Pt/Au Schottky contacts were deposited and defined by lift-off within a circular

opening in the ohmic metal. Electrical characterization was performed on a HP4145 at room temperature on 48 μm diameter diodes. Samples prepared in the same way, except without any metallization, were analyzed with Auger Electron Spectrometry (AES) surface and depth profiles. The surface morphology was also characterized by atomic force microscopy (AFM) before and after annealing.
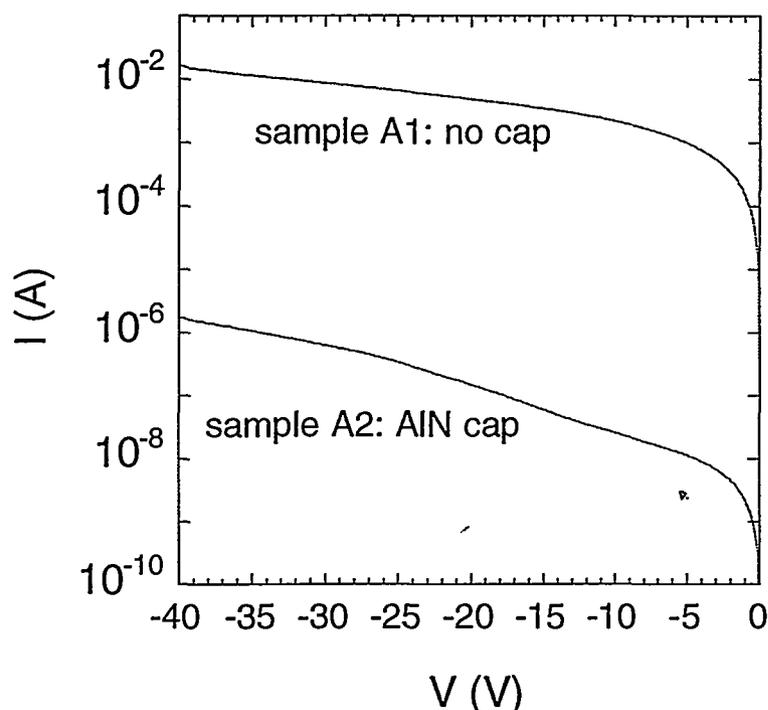
## AlN ENCAPSULATION: RESULTS AND DISCUSSION



Fig 2. Reverse current/voltage characteristics for 48 μm diameter Pt/Au Schottky contacts on GaN annealed at 1100 °C, 15 s with (sample A2) and without (sample A1) an AlN cap.

Figure 2 shows the reverse current/voltage characteristics of 48 μm diameter Pt/Au Schottky diodes on the initially n-type samples. The sample annealed without the AlN cap has over 3 orders-of-magnitude higher reverse leakage current than the capped sample. The implanted samples showed a similar offset in the reverse leakage current between the capped and uncapped samples. The reason for the difference in reverse bias characteristics is discussed below.

Figure 3 shows the current/voltage characteristics between two adjacent Ti/Al ohmic contacts on the same two samples as in Fig 2. Here the sample annealed without the AlN cap displays dramatically lower resistance than the AlN-capped sample. This is consistent with the Schottky characteristics and suggests the creation of an $n^+$-surface layer formed on the sample annealed without the AlN encapsulant.
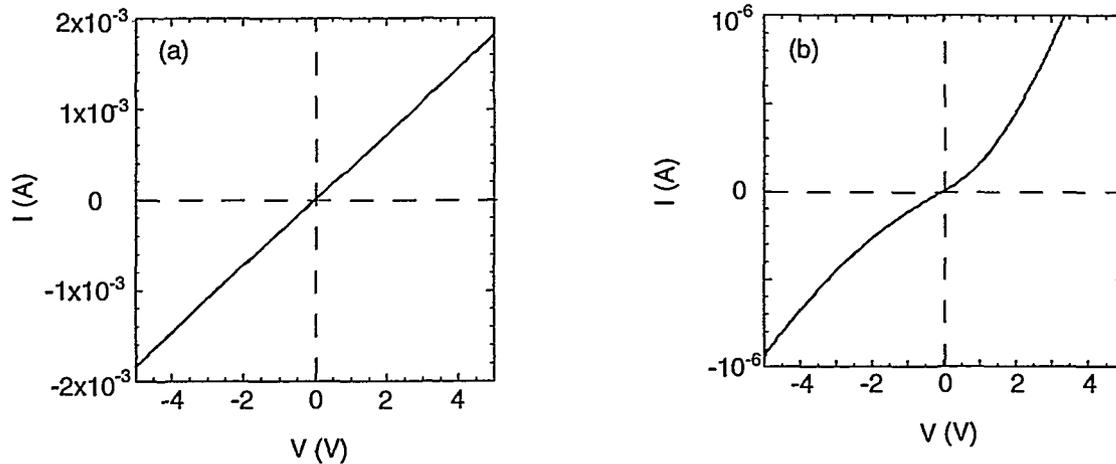
Fig 3. Current/voltage characteristics between two adjacent Ti/Al ohmic contacts on GaN annealed at 1100 °C, 15 s (a) without and (b) with an AlN cap. Note the change in current scale for the two samples.



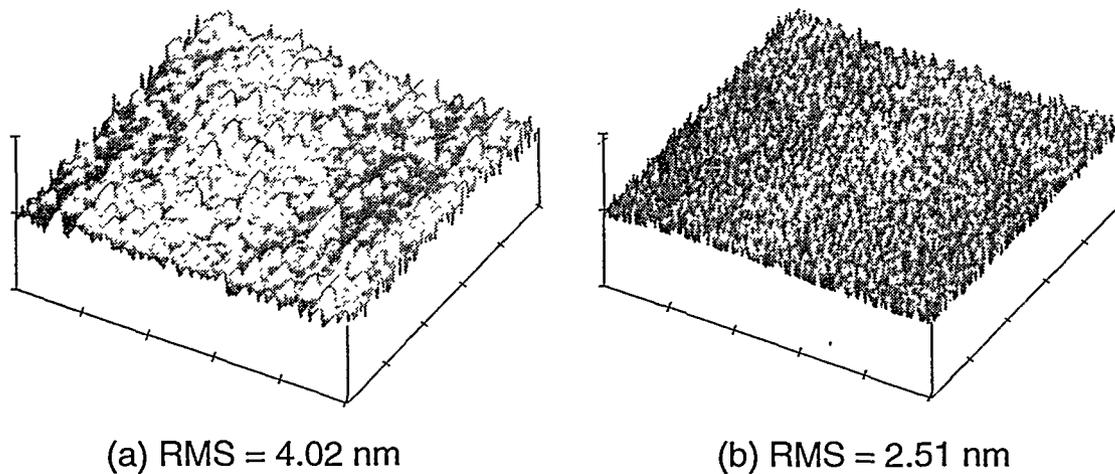(a) RMS = 4.02 nm                    (b) RMS = 2.51 nm

Fig 4. Atomic force microscope images of GaN after an 1100 °C, 15 s anneal either a) uncapped or b) capped with reactively sputtered AlN. The AlN film was removed in a selective KOH-based etch (AZ400K developer) at 60 - 70 °C. On both images, the vertical scale is 50 nm per division and the horizontal scale is 2 μm per division.

Further evidence of the difference between the two annealing processes is seen in the atomic force microscopy images shown in Fig 4. The sample annealed without the AlN cap is markedly rougher than the capped sample, again suggesting some degree of surface decomposition. In an attempt to quantify the change in the GaN surface resulting from annealing with and without the AlN cap, AES surface and depth profiles were performed on

annealed samples (capped and uncapped) after removal of the AlN encapsulant. Unfortunately, it is difficult to compare the absolute Ga and N concentrations from the AES data. However, when comparing the Ga/N ratio for each case we do see an increase for the sample annealed without the AlN cap (Ga/N ratio = 2.34) as compared to the as-grown sample (Ga/N ratio = 1.73). This can be understood by N-loss from the GaN during the annealing process.[29] For the sample annealed with the AlN cap, the AES spectrum had a strong signal from C contamination at the surface that masked the absolute N-concentration. AES depth profiles of the uncapped and annealed sample suggests that the N-loss is occurring in the very near surface region (~ 50 Å).

N-loss and the formation of N-vacancies during the high-temperature anneal is proposed as the key mechanism involved in changing the electrical properties of the Schottky and ohmic contacts. Since N-vacancies are thought to contribute to the background n-type conductivity in GaN, an excess of N-vacancies at the surface should result in a $n^+$-region (possibly a degenerate region) at the surface.[30] This region would then contribute to tunneling under reverse bias for the Schottky diode and explain the increase in the reverse leakage current in the uncapped samples. Similarly, a $n^+$-region at the surface would improve the ohmic contact behavior as seen for the uncapped samples.[31] The effectiveness of the AlN cap during the anneal to suppress N-loss is readily understood by the inert nature of AlN and its extreme thermal stability thereby acting as an effective diffusion barrier for N from the GaN substrate.

## IMPLANTATION DAMAGE AND DOSE EFFECTS

To minimize the access resistance in a transistor structure employing ion implantation such as in Fig 1c,d the implantation dose should be selected at some maximum level determined by dopant solubility and the ability to remove implantation damage. Therefore, it is important to study the activation properties of Si-implanted GaN versus dose.

### Experimental Approach

The GaN layers used in the experiments were 1.5 to 2.0 μm thick grown on c-plane sapphire substrates by metalorganic chemical vapor deposition (MOCVD) in a multiwafer rotating disk reactor at 1040 °C with a ~20 nm GaN buffer layer grown at 530 °C.[32] The GaN layers were unintentionally doped, with background n-type carrier concentrations $\leq 1\times10^{16}$ cm$^{-3}$ as determined by room temperature Hall measurements. When annealed at 1100 °C for 15 s the material maintained its high resistivity. The as-grown layers had featureless surfaces and were transparent with a strong bandedge luminescence at 356 nm at 4 K. Additional luminescence peaks were observed near 378 and 388 nm. We speculate that these second peaks are due to carbon contamination in the film from the graphite heater in the growth reactor. Si ions were implanted at 100 keV at doses from $5\times10^{13}$ cm$^{-2}$ to $1\times10^{16}$ cm$^{-2}$. Ar-ions were implanted at 140 keV and over the same dose range to place its peak range at the equivalent position as the Si. All samples were annealed at 1100 °C for 15 s in flowing N$_2$ with the samples in a SiC-coated graphite susceptor. This annealing sequence has previously been shown to yield activated implanted dopants in GaN.[1,2] Following annealing the samples were characterized at room temperature by the Hall technique by evaporating Ti/Au ohmic contacts at the corners of each sample. Structural analysis of select Si-implanted GaN samples was performed with channeling Rutherford backscatter (C-RBS) and cross-sectional transmission electron microscopy (XTEM).

## Results and Discussion

Figure 5 shows the sheet electron concentrations versus implant dose for the Si and Ar implanted samples after the 1100 °C anneal. For the Si-implanted samples, there appears to be no significant donor activation until a dose of $5 \times 10^{15}$ cm$^{-2}$ is achieved. This is in contrast to earlier results at a dose of $5 \times 10^{14}$ cm$^{-2}$ where roughly 10% of the implanted Si-ions were ionized at room temperature, corresponding to 94% of the implanted Si forming active donors on the Ga-sublattice assuming a Si-donor ionization energy of 62 meV.[1] The lack of free electrons for the lower dose Si-implanted samples in this study may be due to compensation by background carbon in the as-grown GaN as was postulated to exist based on the photoluminescence data. For the two highest dose Si-samples, 5 and $10 \times 10^{15}$ cm$^{-2}$, 35% and 50%, respectively, of the implanted Si-ions created ionized donors at room temperature. The possibility that implant damage alone is generating the free electrons can be ruled out by comparing the Ar-implanted samples at the same dose with the Si-samples which have over a factor of 100 times more free electrons. If the implantation damage were responsible for the carrier generation then the Ar-samples, which will have more damage than the Si-samples as a results of Ar's heavier mass, would demonstrate at least as high a concentration of free electrons as the Si-samples. Since this is not the case, implant damage can not be the cause of the enhanced conduction and the implanted Si must be activated as donors. The significant activation of the implanted Si in the high dose samples and not the lower dose samples is understood based on the need for the Si-concentration to exceed the background carbon concentration that is thought to be compensating the lower dose Si-samples.
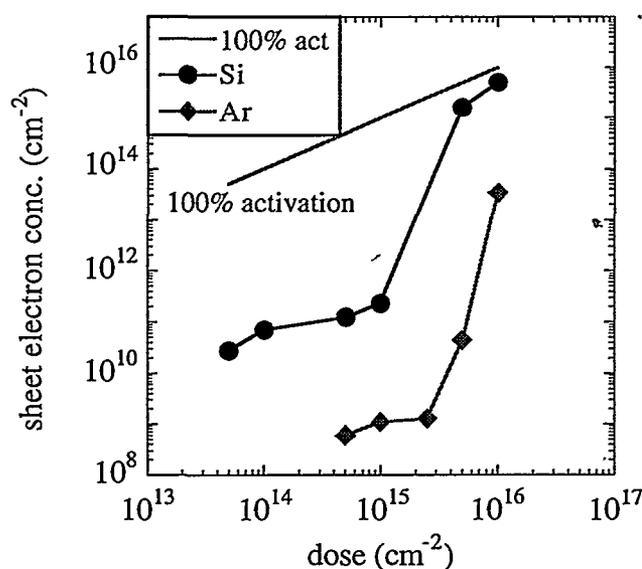


Fig 5. Sheet electron concentration versus implant dose for Si and Ar implanted GaN.

Figure 6 shows the C-RBS spectra for as-implanted (Si: 100 keV, $6 \times 10^{15}$ cm$^{-2}$) and annealed (1100 °C, 30 s) GaN. These figures demonstrate the difficulty in removing the implantation-induced damage from the GaN layer. Although the C-RBS spectra in Fig. 6 displays improved channeling after annealing as seen by the decrease in the backscattered signal, when changes in dechanneling due to the reduced surface peak are accounted for, no significant change in the buried defect concentration is evident.[33] This has been confirmed by the cross-sectional transmission microscopy where the annealed sample still has significant damage apparently consisting of clusters, loops, and planar defects.[33,34] The fact that significant damage remains for an implantation and annealing sequence that produces significant electrical activation of Si-donors as seen in Fig. 5 suggests that complete defect removal is not required to activate implanted Si-donors in GaN. This is in stark contrast to the

case of Si implanted GaAs, where damage removal and dopant activation are sequential processes.[35] However, since the defects in GaN will most likely act as scattering centers and degrade transport properties of the implanted layers, it will be desirable to develop an annealing procedure which more effectively restores the initial crystal quality. This will most likely require using a higher annealing temperature.
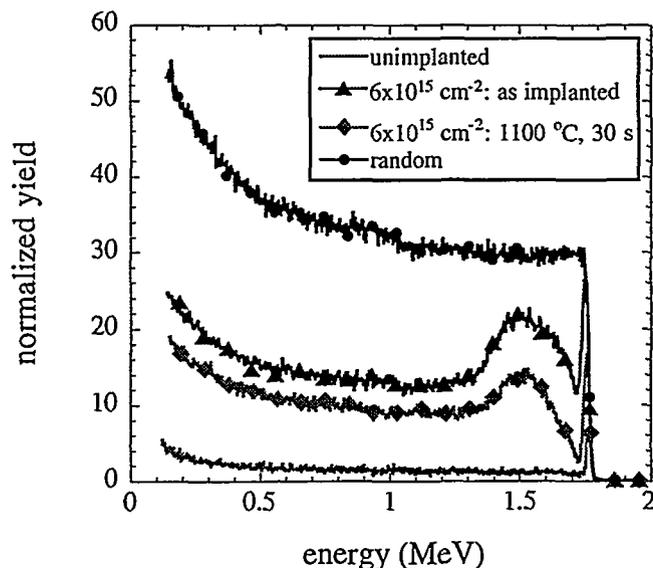


Fig 6. Channeling Rutherford Backscatering spectra of as-implanted (Si: 100 keV, $6 \times 10^{15}$) and annealed at 1100 °C, 30 s.

## CONCLUSION

In conclusion, ion implantation is expected to play an enabling role in the realization of many high performance devices in the III-Nitrides as it has in other mature semiconductor material systems. In particular, ion implantation doping is effective for reducing the access resistance of transistors. Therefore, we have review the progress made in ion implantation doping of GaN with the successful demonstration of n- and p-type doping. The utility of an AlN encapsulating layer was also reported and shown to be effective at maintaining the surface stoichiometry of GaN during the activation anneal and thereby allow the formation of Schottky contact after annealing. It was further shown that high dose Si-implants can be activated up to 50% after a 1100 °C anneal. Finally, C-RBS data was reported that demonstrates the difficulty in removing implantation-induced damage in GaN. However, it appears the complete damage removal is not required to achieve activated implanted Si-donors in GaN. This is sharp contrast to GaAs where donor activation and damage removal are serial processes.

## FUTURE WORK

While significant progress has been made in implantation doping and isolation of GaN, further work remains. In particular, additional work is needed to understand the nature of implantation-induced damage and in developing an annealing sequence to restore the material closer to its as-grown condition. This may require annealing temperatures well in excess of 1100 °C. Other areas of study include implant doping of AlGaN as used in HFET's and continued exploration of alternative p-type dopants.

## References

[1] S. J. Pearton, C. R. Abernathy, C. B. Vartuli, J. C. Zolper, C. Yuan, R. A. Stall, Appl. Phys. Lett. **67**, 1435 (1995).

[2] J. C. Zolper, R. G. Wilson, S. J. Pearton, and R. A. Stall, Appl. Phys. Lett. **68** 1945 (1996).

[3] J. C. Zolper, M. Hagerott Crawford, S. J. Pearton, C. R. Abernathy, C. B. Vartuli, C. Yuan, and R. A. Stall, J. Electron. Mat. **25** 839 (1996).

[4] J. C. Zolper, R. J. Shul, A. G. Baca, R. G. Wilson, S. J. Pearton, and R. A. Stall, Appl. Phys. Lett. **68** 2273 (1996).

[5] S. Nakamura, T. Mukai, M. Senoh, and N. Iwasa, Jap. J. Appl. Phys. **30** L1998 (1991).

[6] S. Nakamura, T. Mukai, M. Senoh, N. Iwasa, and S. Nagahama, Appl. Phys. Lett. **67** 1868 (1995).

[7] S. Nakamura, M. Senoh, S. Nagahama, T. Yamada, T. Matsushita, H. Kiyoku, and Y. Sugimoto, Jap. J. Appl. Phys. **35**, L74 (1996).

[8] S. D. Lester, F. A. Ponce, M. G. Craford, and D. A. Steigerwald, Appl. Phys. Lett. **66** 1249 (1995).

[9] M. A. Khan, A. Bhattarai, J. N. Kuznia, and D. T. Olson, Appl. Phys. Lett. **63**, 1214 (1993).

[10] S. C. Binari, L. B. Rowland, W. Kruppa, G. Kelner, K. Doverspike, and D. K. Gaskill, Elect. Lett. **30**, 1248 (1994).

[11] J. Burm, W. J. Schaff, L. F. Eastman, H. Amano, and I. Akasaki, Appl. Phys. Lett. **68**, 2849 (1996).

[12] Z. Fan, S. N. Mohammad, O. Aktas, A. E. Botchkarev, A. Salador, and H. Morkoc, Appl. Phys. Lett. **69**, 1229 (1996).

[13] Y-F. Wu, B. P. Keller, D. Kapolnek, S. P. Denbaars, and U. K. Mishra, Appl. Phys. Lett. **69**, 1438 (1996).

[14] J. I. Pankove, Tech Digest Inter. Elec. Dev. Meeting, San Francisco, CA, Dec. 11-14, 1994, p. 389.

[15] Gallium Arsenide: Materials Devices, and Circuits: ed. M. J. Howes and D. V. Morgan (John Wiley & Sons, New York, 1985) chapter 10.

[16] S. C. Binari, Proc. of the Sym. Wide Bnadgap Semiconducotrs and Devices, Electrochemical Society, October 8-13, Chicago, IL **vol 95-21**, 136 (1995).

[17] F. Ren, et al. J. Vac Sci. Tech, B, (in press).

[18] I. Akasaki, H. Amano, M. Kito, and K. Hiramatsu, J. Lumin. **48/49** 666 (1991).

[19] S. Strite, Jpn. J. Appl. Phys. **33**, L699 (1994).

[20] A. E. Von Neida, S. J. Pearton, W. S. Hobson, and C. R. Abernathy, Appl. Phys. Lett. **54**, 1540 (1989).

[21] J. C. Zolper, A. G. Baca, and S. A. Chalmers, Appl. Phys. Lett. **62**, 2536 (1993).

[22] J. C. Zolper, M. E. Sherwin, A. G. Baca, and R. P. Schneider, Jr., J. Elec. Mat. **24**, 21 1995).

[23] S. J. Pearton, Inter. J. Modern Physics B, **7**, 4686 (1993).

[24] S. Strite and P. W. Epperlein, Conf. Proc. MRS, Fall 1995, symposium AAA (Material Research Society, Pittsburgh PA, 1996) p. 795.

[25] J. C. Zolper, D. J. Rieger, A. G. Baca, S. J. Pearton, J. W. Lee, and R. A. Stall, "Sputtered AlN Encapsulant for High-Temperature Annealing of GaN," Appl. Phys. Lett. **69**, 538 (1996).

[26] J. R. Mileham, S. J. Pearton, C. R. Abernathy, J. D. MacKenzie, R. J. Shul, and S. P. Kilcoyne, Appl. Phys. Lett. **67**, 1119 (1995).

[27] J. R. Mileham, S. J. Pearton, C. R. Abernathy, J. D. MacKenzie, R. J. Shul, and S. P. Kilcoyne, J. Vac. Sci. Tech. B (in press).

[28] C. B. Vartuli, J. W. Lee, J. D. MacKenzie, S. J. Pearton, C. R. Abernathy, J. C. Zolper, R. J. Shul, F. Ren, Materials Research Society, Boston MA, Dec. 2-6, 1996, in press.

[29] C. D. Thurmond and R. A. Logan, J. Electrochem. Soc. **119**, 622 (1972).

[30] H. P. Maruska and J. J. Tietjen, Appl. Phys. Lett. **15**, 327 (1969).

[31] L. F. Lester, J. M. Brown, J. C. Ramer, L. Zhang, S. D. Hersee, and J. C. Zolper, Appl. Phys. Lett. **69**, 2737 (1996).

[32] C. Yuan, T. Salagaj, A. Gurary, P. Zawadzki, C. S. Chern, W. Kroll, R. A. Stall, Y. Li, M. Schurman, C.-Y. Hwang, W. E. Mayo, Y. Lu, S. J. Pearton, S. Krishnankutty, and R. M. Kolbas, J. Electrochem. Soc. **142**, L163 (1995).

[33] H. H.Tan, J. S. Williams, J. Zou, D. J. H. Cockayne, S. J. Pearton, and C. Yuan, Proc. 1st Symp. on III-V Nitride Materials and Processes, Electrochemcial Society, vol. 96-11, 142 (1996).

[34] J. C. Zolper, H. H. Tan, J. S. Williams, J. Zhou, D. J. H. Cockayne, S. J. Pearton, M. H. Crawford, and R. F. Karlicek, Jr., Appl. Phys. Lett. (submitted).

[35] Ion Implantation and Beam Processing ed. J. S. Williams and J. M. Poate (Academic Press, Sydney, 1984).